Delayed feedback control of collective synchrony: An approach to suppression of pathological brain rhythms

Michael Rosenblum* and Arkady Pikovsky†
Department of Physics, University of Potsdam, PF 601553, D-14415 Potsdam, Germany
(Received 21 May 2004; published 21 October 2004)

We suggest a method for suppression of synchrony in a globally coupled oscillator network, based on the time-delayed feedback via the mean field. Having in mind possible applications for suppression of pathological rhythms in neural ensembles, we present numerical results for different models of coupled bursting neurons. A theory is developed based on the consideration of the synchronization transition as a Hopf bifurcation.

DOI: 10.1103/PhysRevE.70.041904 PACS number(s): 87.19.La, 05.45.Xt

I. INTRODUCTION

Investigation of synchronization in large populations of interacting oscillatory elements is an intensively developing branch of nonlinear science [1–5], relevant to many problems of physics, chemistry, and life sciences, in particular, to neuroscience. For example, synchronization can occur in arrays of lasers and Josephson junctions, where this phenomenon may play a constructive role for generation of a strong coherent field. In other cases synchronization may be harmful; an illustrative example is the excitation of the left-to-right swaying motion of London's Millennium Bridge observed on its opening day.[1] This motion appeared due to mutual synchronization of the steps of hundreds of pedestrians. To prevent the onset of such synchronization, the bridge has been reconstructed in such a way that the damping of its corresponding oscillatory mode was essentially increased. In many cases, when such a direct intervention into the system is not possible, it is nevertheless desirable to control the synchronous motion, in particular, to suppress it, when it appears.

An important example of this class is related to the collective dynamics of neuronal populations. Indeed, synchronization of individual neurons is believed to play the crucial role in the emergence of pathological rhythmic brain activity in Parkinson's disease, essential tremor, and epilepsies; a detailed discussion of this topic and numerous citations can be found in [4,6,7]. Obviously, the development of techniques for suppression of the undesired neural synchrony constitutes an important clinical problem. Technically, this problem can be solved by means of implantation of microelectrodes into the impaired part of the brain with subsequent electric stimulation through these electrodes [8–10]. However, in spite of successful experimental studies followed by clinical applications, the physiological mechanisms of such stimulation remain unclear and the development of effective stimulation techniques is a challenging problem of neuroscience and biological physics. In particular, it is important to minimize the intervention caused by stimulation, e.g., by designing techniques which allow supression of the pathological rhythm by weak though precisely timed pulses [4].

In the present paper we systematically analyze and further develop the time-delayed feedback control of the collective synchrony in a complex oscillator network, suggested in our previous publication [11]. Generally speaking, there are many situations where synchrony appears or disappears with variation of the system parameters, type of coupling, etc. In particular, it is well known that the delayed interaction between two or many oscillators can suppress or facilitate the synchrony [6,12–14], as well as result in oscillation quenching [15,16]. However, these effects of delay are hardly suitable for the purposes of control, because typically the equations and parameters of the system are unknown and cannot be accessed. The advantage of the particular setup of [11] is in the usage of an *external* delayed loop, a few parameters of which (delay time, feedback strength) can be easily controlled by an experimentalist. Contrary to many other problems where a suppression of synchrony has been observed, the suppression with the method considered here requires neither information on the details of the individual oscillators and their interactions nor access to their parameters. Only the macroscopic properties of the collective dynamics determine the feasibility of the control.

We concentrate on a possible application of such a control scheme to suppression of a pathological neural activity. In this respect it is important that after the suppression is achieved the intervention into the system is minimal, i.e., the control is noninvasive. We note that the term "noninvasive" has different meanings in control theory and in neuroscience. Our suppression scheme is noninvasive in the sense that the feedback signal tends to zero, or generally speaking to the noise level, as soon as the suppression is achieved. However, the technique remains invasive in the sense that it requires constant stimulation via implanted electrodes. This "noninvasiveness" is common also for other applications of delayed feedback control, i.e., for stabilization of periodic orbits embedded into a chaotic attractor, suppression of spatial-temporal chaos [17–22], and control of coherence of chaotic systems [23].

The paper is organized as follows. In Sec. II we discuss the current stage of the development of brain stimulation techniques. In Sec. III we describe models of neural oscilla-

*URL: www.agnld.uni-potsdam.de/~mros
†URL: www.stat.physik.uni-potsdam.de/~pikovsky
[1]The corresponding video can be found on the web page of the firm that constructed the bridge: www.arup.com/MillenniumBridge/

tions which we use in the following simulations. Here we also discuss and illustrate the onset of synchrony in neural ensembles. In Sec. IV we present the numerical results illustrating the time-delayed feedback suppression in an ensemble of globally coupled neural oscillators. In Sec. V we present the theoretical description of our approach, as well as a comparison of the theory and of the results of simulations with the models of neural ensembles. Here we also discuss and compare several forms of control. Finally, in Sec. VI we discuss our results and present an outlook.

II. SUPPRESSION OF PATHOLOGICAL BRAIN RHYTHMS BY ELECTRICAL STIMULATION

A. Electrical stimulation of brain structures

For a couple of decades the electrical stimulation of the human brain has been used in pilot studies with the aim of suppressing the pathological activity in epilepsy [8,9] and, with more successful clinical applications, in Parkinson's disease [10]. This surgical procedure, called deep brain stimulation (DBS), involves implanting of an electrode into the subcortical structures for long-term stimulation by a periodic pulse train. In Parkinsonian patients, DBS at frequencies greater than 100 Hz has been shown to relieve tremor as well as other symptoms such as rigidity and dyskinesia. It decreases tremor amplitude in a spectacular way; the illustration of this effect with real data can be found on the PhysioNet web page.[2] The mechanism by which high frequency DBS suppresses tremor and reduces other symptoms in Parkinson's disease is unknown (cf. a discussion in [24]). The parameters of the stimulation must be determined by trial and error and readjusted with time. The efficiency of the DBS is known to decrease with time due to the adaptation of the brain to stimulation.

Another direction of research is related to experiments with brain slices. In this context we mention the feedback controlled dc stimulation reported in [25,26]; it was found that it reduces epileptic activity. The experimentalists conclude that the stimulation changes the parameters of neurons, reducing the excitability threshold.

B. Development of model-based stimulation techniques

The application of nonlinear and statistical methods to DBS has been pioneered by Tass. Sophisticated techniques, currently being developed, imply stimulation by precisely timed pulses and are based on the hypothesized description of the pathological activity in terms of synchronization in a large neuronal population [4,27–32]. In particular, the model of globally (all-to-all) coupled phase oscillators is used. The main idea of the approach is to administer a pulse stimulus which hits the synchronized cluster at a vulnerable phase and in this way desynchronizes it. This final pulse can be preceded by a complex stimulus which entrains or resets the population and thus allows one to determine precisely the time instant for the application of the suppressing pulse. The asynchronous state is unstable, and thus the desynchronized cluster tends to synchronize again; this resynchronization can be blocked by repeatedly delivering the same composite stimulation.

An alternative approach, based on the assumption that global couping coexists with the local one, uses several (four) electrodes that stimulate at different sites with a phase shift $\pi/2$ with respect to each other [32]. In this way, these electrodes entrain subpopulations of neurons, so that four synchronous clusters are formed. When the stimulation is switched off, the clusters desynchronize; after some time the population synchronizes to the one-cluster states again, and stimulation should be switched on again, and so on [32]. Note that this approach goes beyond the model of globally coupled populations and assumes some spatial structure of the network. The details and variants of these techniques can be found in the original publications.

Recently we have shown that collective synchrony in an ensemble of globally coupled oscillators can be efficiently controlled (enhanced or suppressed) by a delayed feedback in the mean field [11]. The efficiency of the control was tested on models of globally coupled Rössler oscillators, as well as of Hindmarsh-Rose and Rulkov models of neuronal oscillators. The ability of a delayed feedback to suppress the collective rhythm suggests that this method might be considered as a possible approach to DBS in the case when a pathological activity arises due to synchrony in a localized neuronal population and can be measured. The discussion and extension of this approach are the main goals of this paper.

III. BASIC MODELS OF NEURAL ENSEMBLES

A. Neural models

Analytical investigations of neuronal synchrony typically exploit simple models of phase oscillators or integrate-and-fire systems. In simulations of the dynamics of neural ensembles it is possible to use more realistic models like the Hodgkin-Huxley one. However, we have to find a compromise between computational efficiency and physiological plausibility. Therefore in this work we use three different neural models, choosing less detailed (but computationally more efficient) models for time consuming simulations, and vice versa.

For the introduction of our technique we have chosen the Hindmarsh-Rose equations [33] which can be considered as a physiologically realistic model of the Hodgkin-Huxley type. The model reads

$$\dot{x} = y - x^3 + 3x^2 - z + 3,$$

$$\dot{y} = 1 - 5x^2 - y,$$

$$\dot{z} = 0.006[4(x + 1.56) - z]. \quad (1)$$

For the chosen parameter values, the solution of the system reminds the irregular (chaotic) bursting of neurons [see Figs. 3(c) and 3(d) below].

In order to model the dynamics of an ensemble of periodically spiking neurons we use the Bonhoeffer–van der Pol model

[2]URL: www.physionet.org/physiobank/database/tremordb/

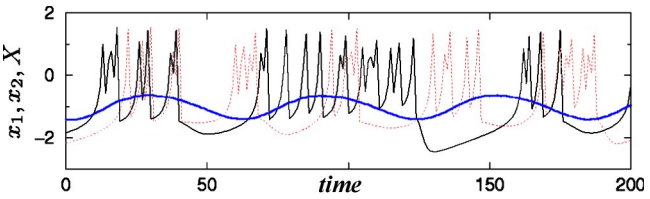

FIG. 1. (Color online) Chaotic bursting of individual neurons in the Rulkov model (3) [time course of two units is shown by solid (black) and dotted (red) lines] and the evolution of the mean field in the globally coupled ensemble of 2000 of such neurons [bold (blue) line].

$$\dot{x} = x - x^3/3 - y + I,$$

$$\dot{y} = 0.1(x + 0.7 - 0.8y). \tag{2}$$

The parameter I has the meaning of the synaptic current and directly influences the spiking frequency.

For detailed numerical analysis of the feedback control of very large ensembles, we have to restrict ourselves to the usage of more simple but computationally efficient models. For this purpose it is very convenient to use the phenomenological model, proposed by Rulkov [34], where a neuron is described by a two-dimensional map:

$$x(n+1) = \frac{4.3}{1 + x^2(n)} + y(n),$$

$$y(n+1) = y(n) - 0.01[x(n) + 1], \tag{3}$$

where n is the discrete time. As follows from Fig. 1 below, each Rulkov neuron exhibits chaotic bursts.

B. Synchrony in neural populations

Pathologically large amplitude brain activity appears due to a coordinated firing of a large number of neurons [4,6,7,35]. In particular, it is hypothesized that collective synchronous dynamics plays a mayor role in the pathology of Parkinson's disease; this viewpoint is partially supported by microelectrode studies [35–38] as well as by analysis of magnetic brain activity (magnetoencephalograms) followed by current source density reconstruction [39,40].

Typically, in a neural population each unit interacts with many other units. The collective dynamics of such a population is usually described by the mean-field model which assumes that the units are globally (all-to-all) coupled [4,6,41,42]. As is well known, for sufficiently strong coupling, such populations undergo the Kuramoto self-synchronization transition [1,2,34,43–49].

Consider an ensemble of N units (with $N \to \infty$ in the thermodynamic limit); coupling within each pair of units is quantified by the parameter K. Each unit can be regarded as driven by the force KX, where $X = N^{-1}\Sigma_{i=1}^{N} x_i$ is the *mean field* and x_i is an observable of the ith unit. The onset of synchronization in the population with the increase of the coupling parameter K beyond a critical value K_c manifests itself via the appearance of nonzero (macroscopic) oscillations of the mean field; on the contrary, the variance of X is small (it vanishes in the thermodynamic limit) if the coupling strength is below the critical value, $K < K_c$. The synchronization transition is often considered in analogy to phase transitions, with the variance of X playing the role of the order parameter [3].

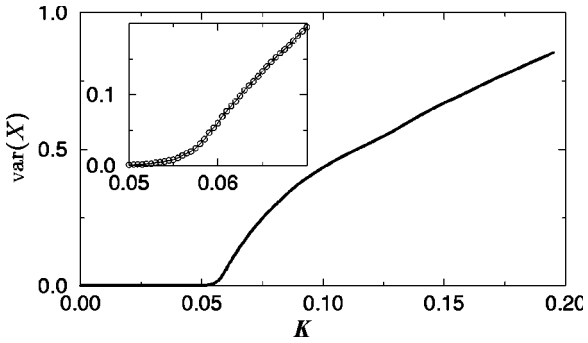

FIG. 2. Transition to the macroscopic mean field in the model (3). The transition is smeared because of the finite-size effect. In the vicinity of the transition point (see inset) the variance of the mean field var(X) increases approximately linearly.

The Kuramoto transition can take place in ensembles of limit cycle oscillators, as in system (2), and also in the presence of noisy perturbations, as well as in ensembles of maps, like (3) and of chaotic oscillators, like (1). The transition can take place also in case of delays τ_{int} in the coupling between the elements of the ensemble. This delay plays an important role in the analysis of neural interactions (see, e.g., [6,12,50]).[3] We illustrate the Kuramoto transition by an example, considering coupled Rulkov models

$$x_i(n+1) = \frac{4.3}{1 + x_i^2(n)} + y_i(n) + KX(n),$$

$$y_i(n+1) = y_i(n) - 0.01[x_i(n) + 1], \tag{4}$$

where $i = 1, \ldots, N$ and

$$X(n) = \frac{1}{N}\sum_{1}^{N} x_i(n).$$

If the coupling K exceeds the critical value $K_c \approx 0.055$, then the neurons start to burst coherently, and a macroscopic mean field appears (see the bold line in Fig. 1 for an example computed for $N = 2000$ and $K = 0.06$).

The evolution of the mean field with K is illustrated in Fig. 2 for $N = 10^4$. We see that in the vicinity of the transition the growth of the variance of the mean field var(X) is approximately linear, as expected for a transition that occurs via the Hopf bifurcation. We note that detailed analysis of the transition for very large ensembles ($N = 10^6$) exhibits that the bifurcation is subcritical. However, the jump at the transition is very small, and therefore it is not seen in the smaller (N

[3] We call this delay *internal* to distinguish it from the delay $\mathcal{T}$ in the control loop, implemented in our technique. Usually $\tau_{int} \ll T$, where T is the period of collective oscillations, while $\mathcal{T}$ can be of order of T or larger. Generally, these two quantities are not related.

$=10^4$) ensemble. Note also that in a finite-size population the mean field is not zero for the subthreshold coupling, but fluctuates with the variance $\sim 1/N$ and the transition is smeared [51].

IV. SUPPRESSION OF COLLECTIVE SYNCHRONY: NUMERICAL ILLUSTRATION

A. Suppression with minimal intervention

For the introduction of the delayed feedback control of collective synchrony we consider suppression of the mean field in an ensemble of $N=10\,000$ identical Hindmarsh-Rose neurons [Eqs. (1)] in the regime of chaotic bursting. The dynamics of the ensemble is described by the following set of equations:

$$\dot{x}_i = y_i - x_i^3 + 3x_i^2 - z_i + 3 + KX + K_f(X(t-\mathcal{T}) - X(t)),$$

$$\dot{y}_i = 1 - 5x_i^2 - y_i,$$

$$\dot{z}_i = 0.006[4(x_i + 1.56) - z_i], \tag{5}$$

where $X=N^{-1}\Sigma_{i=1}^{N} x_i$ is the mean field, and the terms KX and $K_f(X(t-\mathcal{T})-X(t))=\mathcal{C}$ describe the global coupling and the feedback control, respectively.

The results are presented in Fig. 3 for the strength of the internal coupling $K=0.08$. The feedback control was switched on at $t_0=5000$, i.e., $K_f=0$ for $t<t_0$ and $K_f=0.036$ for $t\geqslant t_0$; the delay time is $\mathcal{T}=72.5$. Here the panels (a) and (b) show the mean field and the control signal, respectively. It is clearly seen that switching on of the feedback results in a quick suppression of the mean field in the ensemble, so that only small noiselike fluctuations remain (we recall that the mean field models here the pathological brain activity). It is important that the control signal decays rapidly and then the asynchronous state of the ensemble is maintained by feeding back a very weak signal. Another important feature of the technique is illustrated in the panels (c) and (d) where we show the bursting dynamics of two neurons before (c) and after (d) the feedback was switched on. One can see that the dynamics of individual units barely change; however, they burst incoherently and therefore produce no macroscopic oscillation. Thus, the feedback control suppresses the collective synchrony in the ensemble without suppressing the firing of individual neurons and maintains this state with a weak intervention. Simulations with the Rulkov model [11] demonstrate that the variance of the field fluctuations in the suppressed state decrease with increasing ensemble size as $1/\sqrt{N}$. This means that for very large ensembles the control signal tends to zero, and therefore the control is *noninvasive*.

B. Domains of control

With the previous example we demonstrated that the delayed feedback can be exploited to suppress the mean field oscillation. Now we discuss the influence of the parameters of the control scheme. First of all we emphasize that the control can be organized in different ways. In particular, besides the control term $\mathcal{C}\sim X(t)-X(t-\mathcal{T})$, as in the previous section, one can use control terms in the form of $\mathcal{C}\sim X(t-\mathcal{T})$. We call these delayed feedback schemes *differential* and *direct* control, respectively. In the following we also discuss *multiple delay* control (see Sec. V D). Generally, other forms of control are possible as well, e.g., nonlinear feedback schemes, or feedback schemes using the delayed derivative, and so on.

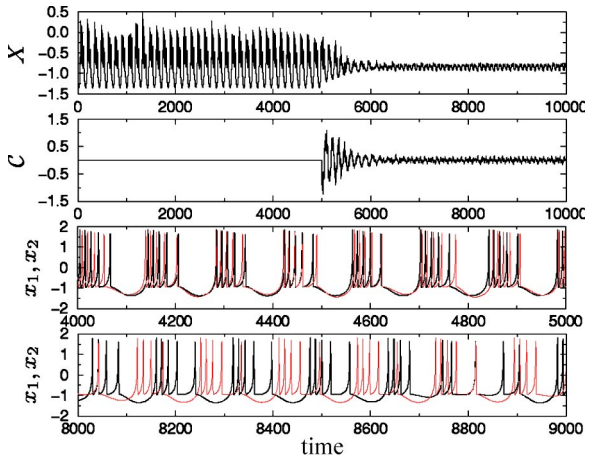

FIG. 3. (Color online) (a) Suppression of the mean field X in the ensemble of 10 000 Hindmarsh-Rose neurons [Eqs. (5)]. The delayed feedback is switched on at $t=5000$. (b) The control signal $\mathcal{C}=\varepsilon_f(X(t-\mathcal{T})-X(t))$ quickly decays to the noise level and the desired, asynchronous, state of the system is maintained with a minimal intervention. (c), (d) Synchronous and asynchronous bursting of two neurons in the absence and in the presence of the feedback, respectively.

Both direct and differential control schemes are parametrized by the delay time $\mathcal{T}$ and the feedback coefficient K_f. Moreover, the phase shift β that determines how the signal acts on the system is also important. We note that $\mathcal{T}$ and K_f can be adjusted in the experimental implementation, and therefore are considered further as free parameters. On the contrary, the phase shift β depends on the way the irradiated control signal influences the individual neurons, and cannot be easily determined. We illustrate the influence of these parameters by the following example.

We consider an ensemble of Bonhoeffer–van der Pol oscillators, coupled via the mean field in the x variable:

$$\dot{x}_i = x_i - x_i^3/3 - y_i + I_i + KX + K_f(\cos\beta)X(t-\mathcal{T}),$$

$$\dot{y}_i = 0.1(x_i + 0.7 - 0.8y_i) - K_f(\sin\beta)X(t-\mathcal{T}). \tag{6}$$

Note that the delayed feedback here generally affects both x and y variables; the relative strength of these actions is governed by the phase shift β. The elements of the ensemble are not identical: the parameter I_i is taken $I_i=0.6+\sigma$, where σ is Gaussian distributed with zero mean and 0.1 rms value. We have performed the simulation of the system (6) for $N=10^4$, for several values of the parameter β, and for regularly varied K_f and $\mathcal{T}$. For each set of parameters we compute the variance of the mean field and the *suppression coefficient* $S=[\mathrm{var}(X)/\mathrm{var}(X_f)]^{1/2}$, where X and X_f are the mean fields in the absence and presence of the feedback, respectively. In the

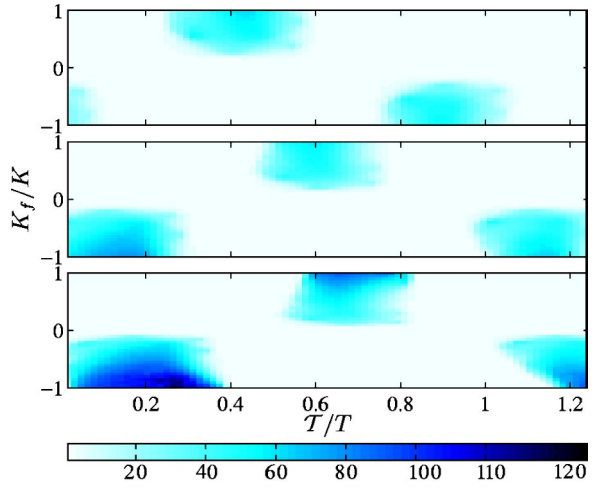

FIG. 4. (Color online) Domains of suppression for the Bonhoeffer–van der Pol ensemble (6). Three panels show the suppression factor S in a gray (color) scale coding. The phase shift β that determines how the control signal acts on the elements of the ensemble changes from top to bottom: $\beta=0$, $-\pi/10$, $-\pi/5$. The delay is normalized by the average period T of the mean-field oscillation without control.

simulation we used $N=10^4$ elements. In Fig. 4 we show the dependence of the suppression coefficient S on $\mathcal{T}$, K_f.

From Fig. 4 we conclude that suppression is observed for relatively large parameter domains, which we call domains of control. The position of these domains along the $\mathcal{T}$ axis depends on the phase shift β; in this example the domains are found around const$+nT/2$, where n is an integer. One can also see that the maximal value of the suppression factor depends on β as well. In the next section we develop a theory that describes the domains of control.

V. SUPPRESSION OF SYNCHRONY IN A GLOBALLY COUPLED ENSEMBLE: THEORY

Qualitatively, the effect of suppression can be explained as follows (for definiteness, we consider now direct feedback): as the mean field X is (approximately) T periodic, then the feedback with $\mathcal{T}\approx nT/2$, $n=1, 2,\ldots$ either reduces or increases, depending on the sign of K_f, the driving to each element of the ensemble. Respectively, this results in a suppression or an enhancement of collective synchrony, quantified by the variance of the mean field.

For the theoretical analysis of the control domains we make use of the fact that the synchronization transition in a globally coupled ensemble can be regarded as a Hopf bifurcation for the mean field. We note, however, that the transition can be more complex (see [52–56]). It is also known that both sub- and supercritical Hopf bifurcations are possible. In the following we consider the most frequent case of the supercritical (soft) bifurcation.

A. The amplitude equation

In order to describe the effect of the time delay on this bifurcation, we first write the model amplitude equation (cf. [2,49]) for the dynamics of the complex mean field A:

$$\dot{A}=(-\varepsilon_c+i\omega')A+(\varepsilon+i\varepsilon')A+(\mathcal{E}+i\mathcal{E}')\mathcal{L}(A(t),A(t-\mathcal{T}))-\zeta'|A|^2A. \tag{7}$$

Here the term $(-\varepsilon_c+i\omega')A$ describes the decay of the mean-field oscillation without the global coupling and delayed feedback, due to the tendency of the ensemble to desynchronize because of a distribution of frequencies and/or noise/chaos in individual elements. The term $(\varepsilon+i\varepsilon')A$ describes the effect of the global coupling; in general the factor $\varepsilon+i\varepsilon'$ is complex. A similar term $(\mathcal{E}+i\mathcal{E}')\mathcal{L}(A(t),A(t-\mathcal{T}))$ describes the effect of the delayed feedback of the mean field; here the operator $\mathcal{L}$ has a different form for different feedback schemes to be considered below. Finally, the last nonlinear term describes the saturation of the mean-field oscillation for large A.

Before proceeding with the analysis of Eq. (7) we discuss the treatment of the delayed term. If the goal of the analysis is the determination of the frequency of a periodic solution, then the delay can be substituted by an equivalent phase shift. However, for the analysis of stability this can be done only if the delay is small compared to the oscillation period and no additional instability appears. The delay in the external feedback loop is not small, and its replacement by the phase shift drastically changes the stability properties. Hence, one should consider a delayed equation which is the infinite-dimensional system. (The same consideration is valid for internal delays, not considered here.)

It is convenient to reduce the number of parameters in Eq. (7), normalizing the time by the frequency of oscillation in the absence of delayed feedback, i.e., by $\omega=\omega'+\varepsilon'$. Then Eq. (7) takes the form

$$\dot{A}=(\xi+i)A+\varepsilon_f e^{-i\alpha}\mathcal{L}(A(t),A(t-\tau))-\zeta|A|^2A. \tag{8}$$

Here the derivative is taken over the dimensionless time $t'=\omega t$ (below we use the old notation for time) and the normalized time delay becomes $\tau=\omega\mathcal{T}$. The parameter $\xi=(\varepsilon-\varepsilon_c)\omega^{-1}$ is the dimensionless growth rate of oscillations, and $\zeta=\zeta'\omega^{-1}$. With these units the period of oscillations of the uncontrolled system is $T=2\pi$. Next, we have introduced the dimensionless feedback factor according to $\varepsilon_f e^{-i\alpha}=(\mathcal{E}+i\mathcal{E}')\omega^{-1}$. Note that the phase shift α is determined by the organization of the global coupling in the ensemble and by the properties of individual units. It is important to mention that even if the internal coupling and the delayed feedback enter the equations in a similar way, as in system (6) with $\beta=0$, the shift α in the corresponding amplitude equation is generally nonzero.

In the following we assume that the coupling is supercritical, $\varepsilon-\varepsilon_c=\xi>0$, i.e., a macroscopic mean field exists. In order to describe the suppression of this field, we should determine which values of the feedback parameters ε_f, τ, and α ensure the stability of the asynchronous state $A=0$ in the controlled system (7). Reduction of the description of the ensemble dynamics to the amplitude equation (8) makes the problem similar to the analysis of the dynamics of a limit cycle oscillator with a delayed feedback [57]. However, the

possibility of such reduction and the ability of the considered delayed feedback to control mean-field oscillations without affecting oscillations of individual units are highly nontrivial. Next, the stability analysis of Eq. (7) remains to be done separately for different $\mathcal{L}(A(t), A(t-\tau))$. Below we consider and compare several types of delayed feedback control $\mathcal{L}(A(t), A(t-\tau))$.

B. Direct control

We start with the control term of the form $\mathcal{L}(A(t), A(t-\tau))=A(t-\tau)$; such a control can be called "direct." In this case the linearized Eq. (8) at the asynchronous state $A=0$ reads

$$\dot{A} = (\xi + i)A + \varepsilon_f e^{-i\alpha} A(t-\tau). \tag{9}$$

In order to analyze the stability of this state we substitute in Eq. (9) $A=A_0 e^{\lambda t}$, and obtain the characteristic equation (cf. [57])

$$\lambda = \xi + i + \varepsilon_f e^{-i\alpha} e^{-\lambda\tau}. \tag{10}$$

The solution of Eq. (10) can be expressed via the Lambert function $W:\mathbb{C}\to\mathbb{C}$, which is defined as the solution of the equation $W(z)e^{W(z)}=z$ [58]. Indeed, rewriting Eq. (10) as

$$\tau(\lambda - \xi - i) = \tau\varepsilon_f e^{-i\alpha} e^{-\lambda\tau}, \tag{11}$$

taking the exponents of both sides, and multiplying by $\tau\varepsilon_f e^{-i\alpha}$, we obtain

$$\tau\varepsilon_f e^{-i\alpha} e^{-(\xi+i)\tau} = \tau\varepsilon_f e^{-i\alpha} e^{-\lambda\tau} e^{\tau\varepsilon_f e^{-i\alpha} e^{-\lambda\tau}}.$$

Comparing with the definition of the Lambert function we obtain $W(\tau\varepsilon_f e^{-i\alpha} e^{-(\xi+i)\tau}) = \tau\varepsilon_f e^{-i\alpha} e^{-\lambda\tau}$, which together with Eq. (11) gives

$$\lambda = \xi + i + \tau^{-1} W(\tau\varepsilon_f e^{-i\alpha} e^{-(\xi+i)\tau}). \tag{12}$$

The condition $\mathrm{Re}(\lambda)<0$ determines the domains of stability on the parameter plane τ, ε_f. (Note that $\lim_{\tau\to 0}\lambda = \xi + i + \varepsilon_f e^{-i\alpha}$.)

We illustrate the theoretical results in Figs. 5 and 6. First we analyze the dependence of the control domains on the third parameter of the control, namely on the phase angle α. One can see that with increase of α the domains of control are shifted along the τ-axis. The domains are positioned around $\tau=\mathrm{const}+n/2T$, where the constant is α-dependent and vanishes for $\alpha=0$. Note that for $\alpha=\pi/2$ there exists no domain at $\tau\approx 0$, so that the "trivial" feedback without delay does not suffice.[4] Negative values of α result in the shift of the control domains to larger delays, in accordance with the numerical results shown in Fig. 4. [We recall that if the phase shift β in Eqs. (6) is zero, the effective phase shift is generally nonzero. This explains why the control domain in the upper panel of Fig. 4 is shifted with respect to $\tau=T/2$.]

Next, we analyze the impact of the only parameter of the (normalized) model equation that characterizes the controlled system, namely, the (normalized) increment ξ. It describes how far the ensemble is from the transition point. As expected, the more unstable is the system, the fewer domains of suppression exist and the smaller they are (see Fig. 6). The possible number of domains is estimated in the Appendix.

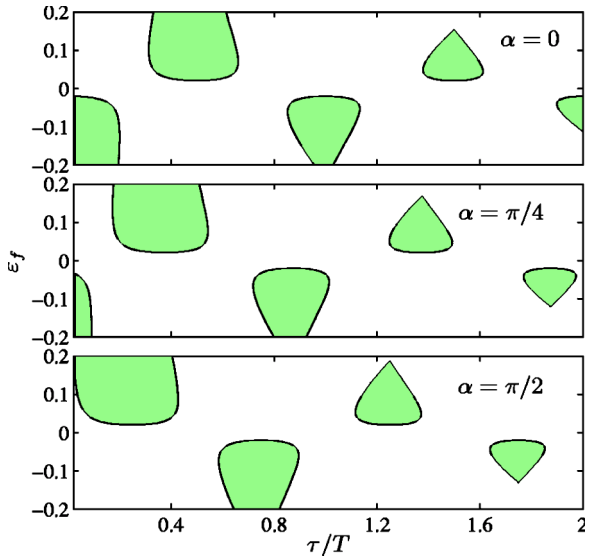

FIG. 5. Domains of control for the direct control scheme, for different phase shift α and constant normalized increment $\xi=0.02$. T is the period of mean-field oscillation in the absence of the feedback.

For the (semi)quantitative comparison of the theoretical description within the framework of the model equation (8) with the numerics we consider the Rulkov model (4) with the control term $K_f X(n-T)$ added to the right-hand side of the first equation. We compute the variance of the mean field for three values of the internal coupling, $K=0.056$, $K=0.06$, K

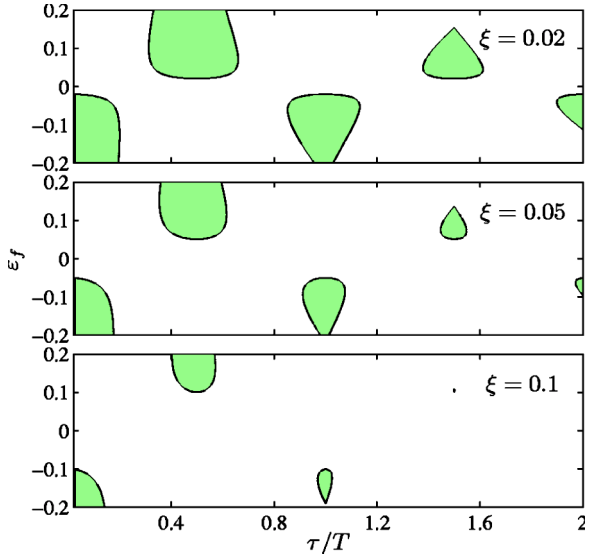

FIG. 6. Domains of control for the direct control scheme in dependence on the stability of the system for constant phase shift $\alpha=0$. The larger is the instability of the system, the smaller are the domains of control and the stronger feedback is required: suppression of synchrony is possible for $|\varepsilon_f| \geq \xi$.

[4]Indeed, with the no-delay feedback the critical value of ε_f providing suppression is given by $\varepsilon_f=-\xi/\cos\alpha$, i.e., $\varepsilon_f\to\pm\infty$ with $\alpha\to\pi/2$.

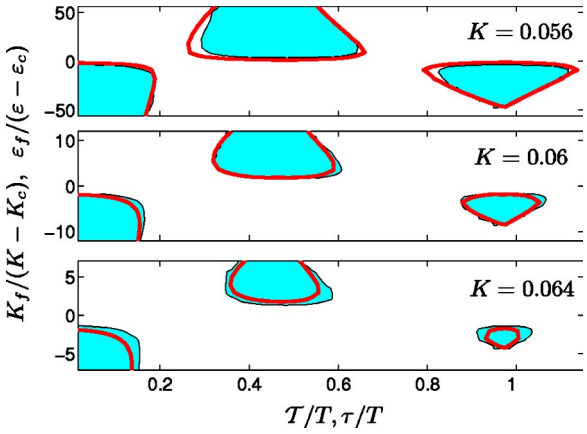

FIG. 7. (Color online) Comparison of the numerical analysis of the stability domains of the feedback controlled Rulkov model (3) (filled regions) with the stability domains for the equivalent model equation (8) [bold (red) lines] for three different values of the internal coupling K (see text).

$=0.064$, and for a range of feedback parameters $\mathcal{T}, K_f$. The size of the ensemble is $N=10^4$. Next, from Fig. 2 we estimate the level of noise in the system, i.e., the variance of the mean field for subcritical coupling, to be 0.003. We use this value as a cutoff level: if the variance of the mean field is larger than this value, the system is considered to be unstable. The obtained stability domains are shown as filled regions in Fig. 7. Next we have to estimate the parameters of the equivalent model equation for the Rulkov model (3). From the bifurcation curve (Fig. 2) we estimate the critical coupling as $K_c = 0.055$. The frequency of the mean field can be easily estimated as $\omega = 2\pi/60$. Taking the increment in the model equation proportional to subcriticality in the full model, i.e., $c\xi = K - K_c$, we finish with two unknown parameters of the model equation that should be determined by a fit. These parameters are c and the equivalent phase shift α. This can be easily done, because these parameters determine the positions of the stability domains along the vertical and horizontal axes, respectively. The results for $c=1.8$ and $\alpha = \pi/18$ shown in Fig. 7 by bold (red) lines demonstrate a good correspondence of the theory and numerics.

To conclude the consideration of the direct control scheme, we discuss whether the controlled system can exhibit bistability. Indeed, generally speaking, for some parameter values the stable asynchronous and synchronous solutions can coexist (see [11]). To analyze this, we look for the domain of existence of the periodic solution $\mathrm{Re}^{i\omega_0 t}$. Substituting this expression into Eq. (8) with the control term as in Eq. (9), we obtain

$$\zeta R^2 = \xi + \varepsilon_f \cos(\omega_0 \tau + \alpha),$$

$$1 = \omega_0 + \varepsilon_f \sin(\omega_0 \tau + \alpha). \tag{13}$$

The periodic solution exists if $R^2 \geqslant 0$, which leads to the equations for the border of the domain [cf. Eqs. (A2)]. Thus we can conclude that there is no bistability in the system, and within the domains of control the mean-field oscillations can always be suppressed.

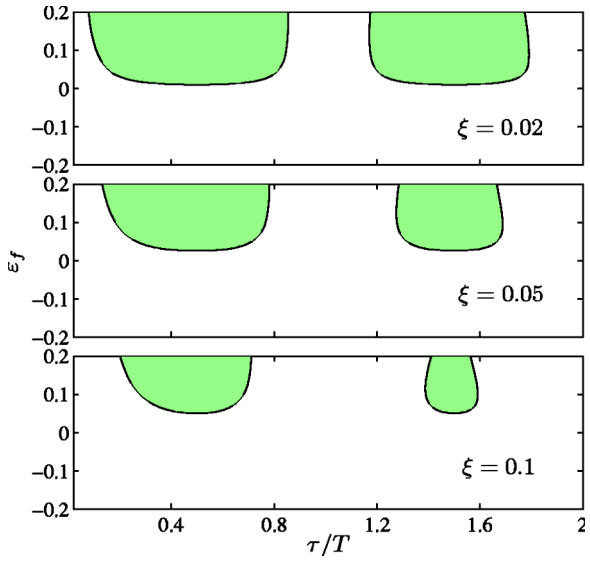

FIG. 8. Domains of control for the differential control scheme, for different ξ; $\alpha=0$.

C. Differential control

In this section we consider Eq. (8) with the differential control term $\mathcal{L}(A(t), A(t-\tau)) = A(t-\tau) - A(t)$ resulting in the linearized equation

$$\dot{A} = (\xi + i)A + \varepsilon_f e^{-i\alpha}[A(t-\tau) - A(t)]. \tag{14}$$

Note that such a control is used in the Pyragas method of chaos suppression; there it is important that τ equals the period of an unstable periodic orbit of the chaotic attractor, while in our case τ is a free parameter. The normalized characteristic equation reads

$$\lambda = \xi + i + \varepsilon_f e^{-i\alpha}(e^{-\lambda\tau} - 1), \tag{15}$$

and its solution is expressed via the Lambert function as

$$\lambda = \xi - \varepsilon_f \cos\alpha + i(1 + \varepsilon_f \sin\alpha) + \tau^{-1} W(\tau\varepsilon_f e^{-i\alpha} e^{-[\xi - \varepsilon_f \cos\alpha + i(1+\varepsilon_f \sin\alpha)]\tau}). \tag{16}$$

The domains of control are shown in Figs. 8 and 9. Comparing the results for direct and differential control schemes, we mention (i) for small α the differential control provides larger domains of control; however, the number of domains is smaller as the control can be performed for positive feedback only; (ii) for α close to $\pi/2$ both the direct and the differential schemes are approximately equally effective with regard to the parameter range where control is possible; (iii) similarly to the direct control, the differential scheme provides no bistability.

In order to conclude the comparison of the two schemes, we shall determine the degree of stability within the domains of control; the latter is quantified by the absolute value of λ. Indeed, in the presence of noise the "depth" of the stability domain determines the variance of the fluctuations in the suppressed state. This comparison is shown in Fig. 10. We see that for small α the differential control provides stronger stability.

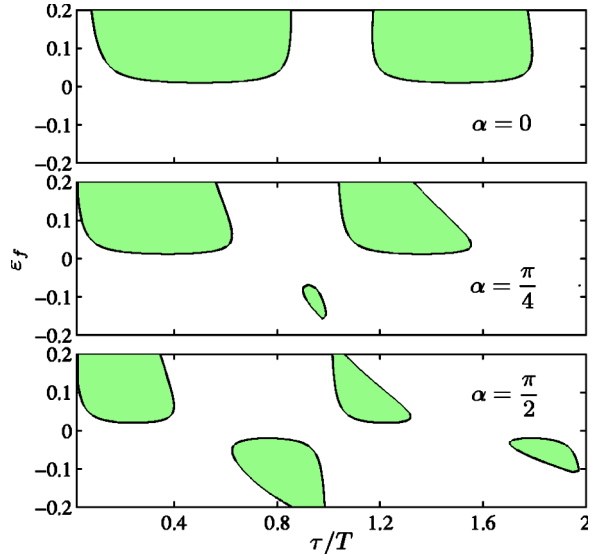

FIG. 9. Domains of control for the differential control scheme, for different α; $\xi=0.02$.

D. Multiple-delay control

In this section we explore whether we can improve suppression of collective synchrony by exploiting multiple-delay control. For this purpose we modify the multiple-delay version of the Pyragas control suggested by Socolar *et al.* [59]. We write the control term as $\mathcal{L}=B(t-\tau)$, where the auxiliary signal $B(t)$ obeys

$$B(t) = (1-\mu)A(t) + \mu B(t-\tau_m), \tag{17}$$

here the delay τ_m and coefficient $0<\mu<1$ are free parameters. Implementation of such a control requires two delay lines: the mean field A should be stored on the interval $t-\tau$, and the auxiliary signal $B(t)$ should be stored on the interval $t-\tau_m-\tau$.

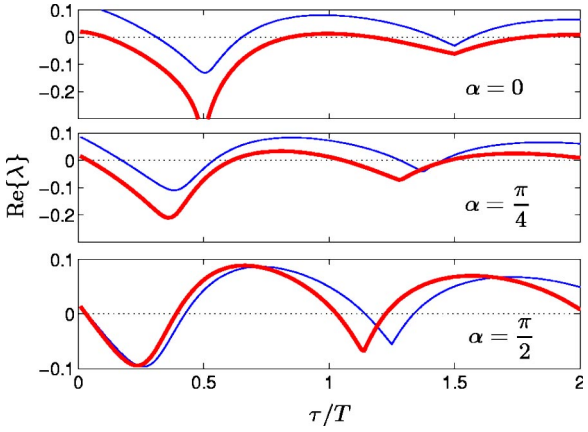

FIG. 10. Profiles of λ for direct (solid) and differential (bold) control scheme; $\xi=0.02$, $\varepsilon_f=0.1$.

The control scheme (17) is equivalent to a control with infinitely many delay lines. Indeed, substituting $B(t-\tau_m)$ in the expression (17) and iterating such substitutions, we obtain

$$B(t-\tau) = (1-\mu)[A(t-\tau) + \mu A(t-\tau_m-\tau) + \mu^2 A(t-2\tau_m-\tau) + \mu^3 A(t-3\tau_m-\tau) + \cdots].$$

The characteristic equation of the linearized Eq. (8) takes the form

$$\lambda = \xi + i + \varepsilon_f e^{-i\alpha} e^{-\lambda\tau}(1-\mu)(1+\mu e^{-\lambda\tau_m} + \mu^2 e^{-2\lambda\tau_m} + \cdots) = \xi + i + \frac{\varepsilon_f(1-\mu)e^{-i\alpha-\lambda\tau}}{1-\mu e^{-\lambda\tau_m}}. \tag{18}$$

The solution of this equation cannot be expressed in terms of the Lambert function. Introducing the notation $\lambda=\gamma+i\varphi$ and separating real and imaginary parts we find the solution of Eq. (18) in a parametric form:

$$\tau = \varphi^{-1}\left[\arctan\left(\frac{(\varphi-1)[\mu e^{-\gamma\tau_m}\cos(\varphi\tau_m)-1] - (\gamma-\xi)\mu e^{-\gamma\tau_m}\sin(\varphi\tau_m)}{(\gamma-\xi)[1-\mu e^{-\gamma\tau_m}\cos(\varphi\tau_m)] - (\varphi-1)\mu e^{-\gamma\tau_m}\sin(\varphi\tau_m)}\right) + n\pi - \alpha\right],$$

$$\varepsilon_f = e^{\gamma\tau}\frac{(\gamma-\xi)[1-\mu e^{-\gamma\tau_m}\cos(\varphi\tau_m)] - (\varphi-1)\mu e^{-\gamma\tau_m}\sin(\varphi\tau_m)}{(1-\mu)\cos(\varphi\tau+\alpha)}. \tag{19}$$

Setting $\gamma=0$ we obtain the borders of control domains. The results are shown in Fig. 11. For better comparison, in the upper panel we show the domains for $\mu=0$, i.e., for the one-delay direct control scheme. The bold (red), solid (blue), and dashed (black) contour lines correspond to $\mathrm{Re}(\lambda)=0,-0.1$, and -0.2, respectively. In the lower panel we show the similar contour lines for $\mu=0.3$; other parameters are the same for the two cases: $\xi=0.1, \alpha=0$. We see that control can be indeed enhanced by using multiple delays, although the improvement is not drastic.

VI. DISCUSSION AND OUTLOOK

In this paper we considered in detail the suppression of the mean field in an ensemble of oscillators from the viewpoint of a possible application in neuroscience. Particularly,

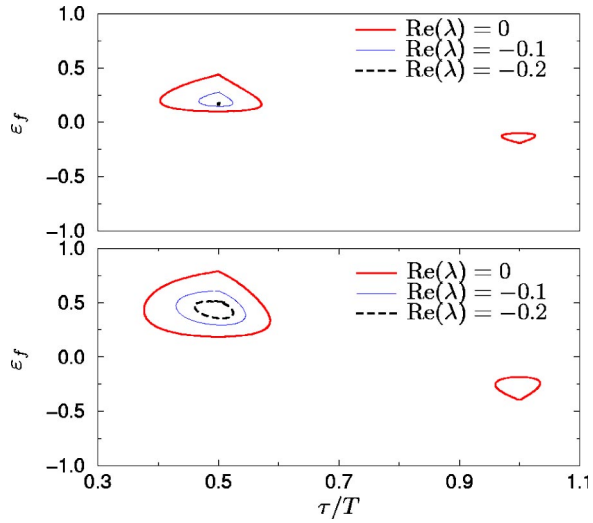

FIG. 11. Efficiency of the multiple-delay control scheme. Upper panel shows the borders of two control domains for the one-delay direct control scheme [bold (red) lines]. Lower panel shows these borders for the multiple-delay control. Solid (blue) and dashed (black) contour lines correspond to $\mathrm{Re}(\lambda)=-0.1$ and -0.2. Note that the second delay makes the control domains larger and more "deep."

we suggest that time-delayed feedback can be used for the purposes of deep brain stimulation, namely, for suppression of pathological brain rhythms. The final goal is the development of a device that will implement such a control via microelectrodes implanted into the brain. More realistically, we hope that the technique will be of interest to neuroscientists working on neural oscillations in brain slices. We support our idea by numerical simulation of the ensemble dynamics using mathematical neuronal models of different complexity, as well as by a theoretical treatment. In our consideration we exploited the idealized model of globally coupled neurons; however, numerical analysis of randomly coupled networks indicates that our approach works in this case as well (this study will be reported elsewhere). Also, the method works even when the interaction between units involves some retardation due to the finite velocity of the signal transmission between neurons [6,12,13]. We note that we did not analyze in detail the influence of the different types of interaction between individual units of the network, which may be of chemical or electrical origin, and may occur via the gap junctions or via synapses. Properties of the coupling are certainly important for a quantitative description of the synchronization transition in a network; however, this transition generally occurs via the Hopf bifurcation and therefore we believe that our technique is applicable for different types of neuronal interaction.

We have performed a comparative analysis of two control schemes that we call direct and differential control. The important difference between these two techniques is that the first one is generally invasive, in the sense that the control signal in the suppressed state tends to a constant, whereas the latter technique is noninvasive, i.e., the control tends to zero. (In a noisy ensemble of finite size this means that the control signals fluctuate around a constant or zero, respectively.) The possibility to implement the noninvasive control is very important from the viewpoint of practical implementation of this approach. Indeed, for noninvasive control the signal that is fed into the system is large only for a rather short time (cf. Fig. 3), before the mean-field oscillation is suppressed. After this, the signal that is required to maintain the normal state of the neuronal network has the level of noisy fluctuations in the system. Hence, the feedback control can be exploited for long periods of time, because both the intervention into the tissue and energy consumption from the device battery are minimized. Next, we have shown that using two delay lines one can improve the efficiency of the control, by enlarging the control domains in the parameter plane and by achieving stronger stability of the desynchronized state within these domains.

Another advantage of the delayed-feedback suppression is that this scheme allows one to easily overcome the effect known in engineering as latency. Indeed, in a practical application it can happen that the mean field is registered with some retardation time τ_m. For example, the collective rhythm of a neuronal population could be more conveniently measured by surface electrodes. In this case the measured signal can be a delayed version of the local electric field due to finite conduction velocity along the neural pathways. Clearly, the suppression will work in this case as well; the delay time in the external feedback loop should be chosen in such a way that the resulting delay $\tau+\tau_m$ lies within a domain of suppression. There is another issue of practical importance: usually the observed mean field (local field potential as it is called in neurodynamics) has to be filtered before being used for feedback control. We expect that such a filtering does not significantly reduce the feasibility of the control; however, this aspect needs special consideration, to be reported elsewhere.

In our discussion of the pathological synchrony in a subsystem of the brain we followed the commonly accepted approach that this synchrony (and, hence, pathological activity) develops due to an increase of the interneuron coupling (parameter K in our models). We recall now that for certain parameters the delayed feedback can cause a reverse effect and bring instability into a stable ensemble, thus enhancing the mean-field oscillation (see [11]). We speculate that this effect might be a cause of a pathological brain activity: the neural network where this activity is generated cannot be considered as isolated from other regions of the brain. Indeed, this network receives the signals from other functional subsystems of the central and peripheral neural systems. In particular, there are some natural, internal feedback loops characterized by their own amplifications and delays. We can assume that some (pathological) change of the parameters of these loops can result in excitation of mean-field oscillation. This would mean that suppression of pathological rhythms can be achieved by affecting (e.g., by a medication) these internal loops.

To conclude, we mention some directions of ongoing research. A practical method for determination of the appropriate parameters of the feedback control $\mathcal{T}$ and K in a real experiment is still lacking. A possible solution here might be implementation of a nonlinear optimization scheme. Next, an important extension of the presented technique would be

consideration of the spatial effects that are neglected in the model of global coupling. For practical implementation it is also necessary to analyze in detail the suppression of multimode instabilities. Indeed, generally, an ensemble of globally coupled elements can have many modes of instability [6]; moreover, the delayed feedback may bring new instability. Preliminary analysis of the delayed-feedback control in an ensemble of noisy phase oscillators [11] shows that the stability of different modes can be treated separately, and the domains of overall stability can be obtained as the intersections of the stability domains for all modes. A very important topic of future study is a comparison and possibly a combination of this approach with the phase resetting techniques developed by Tass [4,27–32].

ACKNOWLEDGMENTS

The work has been supported by DFG (SFB 555 "Complex nonlinear processes"). The authors gratefully acknowledge discussions with O. Popovych and P. A. Tass.

APPENDIX: ESTIMATION OF THE NUMBER OF CONTROL DOMAINS

In order to estimate the number of domains for the given parameters of the characteristic equation (here we take $\alpha=0$)

$$\lambda = \xi + i + \varepsilon_f e^{-\lambda\tau}, \tag{A1}$$

we write $\lambda = i\nu$ and obtain two real equations for the borders of the stability domains (see [57]):

$$\varepsilon_f \cos \nu\tau = -\xi,$$

$$\varepsilon_f \sin \nu\tau = 1-\nu. \tag{A2}$$

Squaring and summing these equations gives $\varepsilon^2=\xi^2+(1-\nu)^2$. Dividing the equations gives $\tan \nu\tau=(\nu-1)/\xi$. Considering separately the cases $1 \geqslant \nu$ and $1<\nu$, we end with the expression for two border lines (they describe two modes of instability)

$$\tau = \frac{\arctan(\mp\sqrt{\varepsilon_f^2-\xi^2}/\xi)+n\pi}{1-\sqrt{\varepsilon_f^2-\xi^2}}.$$

Let us now find the maximal number of suppression regions. To do this, note that a region disappears if both border lines [which can be described by some functions $\tau=f_{1,2}(\varepsilon_f)$] have at the tip of the region, i.e., in the points $\varepsilon_f=|\xi|$, the derivative $d\tau/d\varepsilon_f=0$. The following relations are satisfied at the tip: $\nu=1$, $\tau/T=n/2$, where $n=0$, 1, …, or $\tau\omega=n\pi$. To find the derivative, let us derive Eqs. (A2) with respect to ε_f. We get

$$\cos \nu\tau - e_f \sin \nu\tau\left(\frac{d\nu}{d\varepsilon_f}\tau+\nu\frac{d\tau}{d\varepsilon_f}\right)=0,$$

$$\sin \nu\tau + e_f \cos \nu\tau\left(\frac{d\nu}{d\varepsilon_f}\tau+\nu\frac{d\tau}{d\varepsilon_f}\right)=-\frac{d\nu}{d\varepsilon_f}. \tag{A3}$$

Multiplication of the first equation by cosine and the second by sine and summation yields

$$1=-\frac{d\nu}{d\varepsilon_f}\sin \nu\tau.$$

Then from the first equation we get

$$\cos \nu\tau + \varepsilon_f\tau - \varepsilon_f \sin(\nu\tau)\nu\frac{d\tau}{d\varepsilon_f}=0.$$

Finally, we obtain

$$\frac{d\tau}{d\varepsilon_f}=\frac{\cos \nu\tau+\varepsilon_f\tau}{\varepsilon_f\nu\sin \nu\tau}.$$

The required condition is then $\cos \nu\tau+\varepsilon_f\tau=0$, or, if we take into account the values at the tip, $\tau\xi=\pi n\xi=1$. Hence, suppression is possible for the number of regions $N_r=[(\pi\xi)^{-1}]$, where [ ] denotes the integer part.

[1] A. T. Winfree, *The Geometry of Biological Time* (Springer, Berlin, 1980).
[2] Y. Kuramoto, *Chemical Oscillations, Waves and Turbulence* (Springer, Berlin, 1984).
[3] H. Haken, *Advanced Synergetics: Instability Hierarchies of Self-Organizing Systems* (Springer, Berlin, 1993).
[4] P. A. Tass, *Phase Resetting in Medicine and Biology: Stochastic Modelling and Data Analysis* (Springer, Berlin, 1999).
[5] A. Pikovsky, M. Rosenblum, and J. Kurths, *Synchronization: A Universal Concept in Nonlinear Sciences* (Cambridge University Press, Cambridge, England, 2001).
[6] D. Golomb, D. Hansel, and G. Mato, in *Neuro-informatics and Neural Modeling*, Handbook of Biological Physics Vol. 4, edited by F. Moss and S. Gielen (Elsevier, Amsterdam, 2001), pp. 887–968.
[7] *Epilepsy as a Dynamic Disease*, edited by J. Milton and P. Jung (Springer, Berlin, 2003).
[8] S. A. Chkhenkeli, Bull. Georgian Acad. Sci. **90**, 406 (1978).
[9] S. A. Chkhenkeli, in *Epilepsy as a Dynamic Disease* (Ref. [7]), pp. 249–261.
[10] A. Behabid *et al.*, Lancet **337**, 403 (1991).
[11] M. G. Rosenblum and A. S. Pikovsky, Phys. Rev. Lett. **92**, 114102 (2004).
[12] M. K. S. Yeung and S. H. Strogatz, Phys. Rev. Lett. **82**, 648 (1999).
[13] E. Niebur, H. G. Schuster, and D. M. Kammen, Phys. Rev. Lett. **67**, 2753 (1991).
[14] M. Dhamala, V. K. Jirsa, and M. Ding, Phys. Rev. Lett. **92**, 074104 (2004).
[15] D. V. Ramana Reddy, A. Sen, and G. L. Johnston, Phys. Rev. Lett. **80**, 5109 (1998).
[16] D. V. Ramana Reddy, A. Sen, and G. L. Johnston, Phys. Rev.

Lett. **85**, 3381 (2000).
[17] K. Pyragas, Phys. Lett. A **170**, 421 (1992).
[18] K. Pyragas, Phys. Lett. A **206**, 323 (1995).
[19] G. Franceschini, S. Bose, and E. Schöll, Phys. Rev. E **60**, 5426 (1999).
[20] M. Bertram and A. S. Mikhailov, Phys. Rev. E **63**, 066102 (2001).
[21] P. Parmananda, Phys. Rev. E **67**, 045202(R) (2003).
[22] W. Just *et al.*, Phys. Rev. E **67**, 026222 (2003).
[23] D. Goldobin, M. Rosenblum, and A. Pikovsky, Phys. Rev. E **67**, 061119 (2003).
[24] M. S. Titcombe, L. Glass, D. Guehl, and A. Beuter, Chaos **11**, 766 (2001).
[25] B. J. Gluckman *et al.*, J. Neurophysiol. **76**, 4202 (1996).
[26] B. J. Gluckman, H. Nguyen, S. L. Weinstein, and S. J. Schiff, J. Neurosci. **21**, 590 (2001).
[27] P. A. Tass, Europhys. Lett. **53**, 15 (2001).
[28] P. A. Tass, Europhys. Lett. **55**, 171 (2002).
[29] P. A. Tass, Phys. Rev. E **66**, 036226 (2002).
[30] P. A. Tass, Europhys. Lett. **57**, 164 (2002).
[31] P. A. Tass, Biol. Cybern. **87**, 102 (2002).
[32] P. A. Tass, Biol. Cybern. **89**, 81 (2003).
[33] J. L. Hindmarsh and R. M. Rose, Proc. R. Soc. London, Ser. B **221**, 87 (1984).
[34] N. F. Rulkov, Phys. Rev. Lett. **86**, 183 (2001).
[35] H. Bergman *et al.*, Trends Neurosci. **21**, 32 (1998).
[36] M. Magnin, A. Morel, and D. Jeanmonod, Neuroscience **96**, 549 (2000).
[37] J. Sarnthein, A. Morel, A. von Stein, and D. Jeanmonod, Thalamus Relat. Syst. **2**, 321 (2003).
[38] J. A. Goldberg *et al.*, J. Neurosci. **24**, 6003 (2004).
[39] P. Tass *et al.*, Phys. Rev. Lett. **81**, 3291 (1998).
[40] P. A. Tass *et al.*, Phys. Rev. Lett. **90**, 088101 (2003).
[41] D. Hansel and H. Sompolinsky, Phys. Rev. Lett. **68**, 718 (1992).
[42] P. C. Bressloff, Phys. Rev. E **60**, 2160 (1999).
[43] Y. Kuramoto, in *International Symposium on Mathematical Problems in Theoretical Physics*, edited by H. Araki, Springer Lecture Notes Phys., Vol. 39 (Springer, New York, 1975), p. 420.
[44] R. Mirollo and S. Strogatz, SIAM (Soc. Ind. Appl. Math.) J. Appl. Math. **50**, 1645 (1990).
[45] A. Pikovsky, M. Rosenblum, and J. Kurths, Europhys. Lett. **34**, 165 (1996).
[46] S. H. Strogatz, Physica D **143**, 1 (2000).
[47] D. Topaj, W.-H. Kye, and A. Pikovsky, Phys. Rev. Lett. **87**, 074101 (2001).
[48] E. Ott, P. So, E. Barreto, and T. Antonsen, Physica D **173**, 29 (2002).
[49] J. D. Crawford, J. Stat. Phys. **74**, 1047 (1994).
[50] N. Brunel and V. Hakim, Neural Comput. **11**, 1621 (1999).
[51] A. Pikovsky and S. Ruffo, Phys. Rev. E **59**, 1633 (1999).
[52] H. Daido, Prog. Theor. Phys. **88**, 1213 (1992).
[53] H. Daido, Prog. Theor. Phys. **89**, 929 (1993).
[54] H. Daido, J. Phys. A **28**, L151 (1995).
[55] H. Daido, Physica D **91**, 24 (1996).
[56] J. D. Crawford, Phys. Rev. Lett. **74**, 4341 (1995).
[57] D. V. Ramana Reddy, A. Sen, and G. L. Johnston, Physica D **144**, 335 (2000).
[58] R. M. Corless *et al.*, Adv. Comput. Math. **5**, 329 (1996).
[59] J. E. S. Socolar, D. W. Sukow, and D. J. Gauthier, Phys. Rev. E **50**, 3245 (1994).